Enhancing Sensitivity of SPR Biosensors by Functionalized Gold Nanoparticles – Size Matters.

ARTICLE *in* ANALYTICAL CHEMISTRY · SEPTEMBER 2014

Impact Factor: 5.64 · DOI: 10.1021/ac502637u · Source: PubMed

5 AUTHORS, INCLUDING:

Maria Laura Ermini
Institute of Photonics and Electronics (IPE)
15 PUBLICATIONS **94** CITATIONS
SEE PROFILE

Barbora Spackova
Institute of Photonics and Electronics (IPE)
11 PUBLICATIONS **116** CITATIONS
SEE PROFILE

Jiri Homola
Institute of Photonics and Electronics (IPE)
199 PUBLICATIONS **12,033** CITATIONS
SEE PROFILE

analytical chemistry

Article

pubs.acs.org/ac

Enhancing Sensitivity of Surface Plasmon Resonance Biosensors by Functionalized Gold Nanoparticles: Size Matters

Tomáš Špringer, Maria Laura Ermini, Barbora Špačková, Jani Jabloňků, and Jiří Homola*

Institute of Photonics and Electronics AS CR, v. v. i., Chaberská 57, 182 51, Prague, Czech Republic

Supporting Information

ABSTRACT: We study how the size of spherical gold nanoparticles (AuNPs) influences their ability to enhance the response of optical biosensors based on surface plasmon resonance (SPR). We present a theoretical model that relates the enhancement generated by the AuNPs to their composition, size, and concentration, thus allowing for accurate predictions regarding the SPR sensor response to various AuNPs. The effect of the AuNP size is also investigated experimentally using an SPR biosensor for the detection of carcinoembryonic antigen (CEA) in which AuNPs covered with neutravidin (N-AuNPs) are used in the last step of a sandwich assay to enhance the sensor response to biotinylated secondary antibody against CEA. The experimental data are in excellent agreement with the results of the theoretical analysis. We demonstrate that the sensor response enhancement generated by the N-AuNPs is determined by (i) the sensor sensitivity to N-AuNP surface density (S_σ) and (ii) the ability of the N-AuNPs to bind to the functionalized surface of the sensor. Our results indicate that, while S_σ increases with the size of the N-AuNP, the ability of the functionalized surface of the sensor to bind the N-AuNPs is affected by steric effects and decreases with the size of N-AuNP.

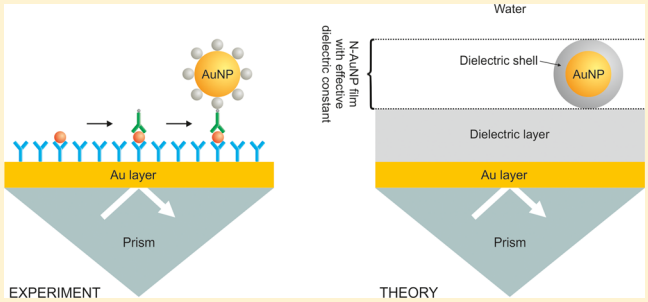

Surface plasmon resonance (SPR) biosensors are among the most advanced label-free optical biosensor technologies and hold potential for applications in numerous important fields, such as medical diagnostics, environmental monitoring, food safety, and security.[1] In order to push for the detection of analytes present at extremely low concentrations, various methods for increasing the sensitivity of SPR biosensors have been developed. Most of these methods are based on changing the refractive index at the sensor surface by means of a variety of (bio)chemical or nanoparticle agents, which are captured by the sensor surface subsequent to the binding of the target analyte to the primary biorecognition elements. These methods include the use of secondary and tertiary antibodies,[2−4] antibodies labeled with enzymes,[5,6] and dielectric[7,8] or metallic nanoparticles (NPs).[6,9−12] In particular, gold spherical nanoparticles (AuNPs) of diameters ranging from 5 to 40 nm have been widely used to enhance the response of SPR biosensors. For instance, Huang et al. used a biotinylated secondary antibody along with 20 nm AuNPs coated with streptavidin to improve the limit of detection (LOD) for prostate-specific antigen in buffer from 10 ng/mL to subng/mL levels.[9] Cao and Sim used a double-enhancement strategy in which AuNPs were coated with HRP-labeled antibody for the detection of PSA down to the subng/mL level.[6] In our recent work, we employed 30 nm AuNPs functionalized with streptavidin to detect carcinoembryonic antigen (CEA) in 50% blood plasma down to a 0.1 ng/mL level.[10] Despite this rather broad use of AuNPs in SPR biosensors, there is a lack of quantitative data describing the influence of the size of AuNPs on the outcome of the detection.[13,14]

Previous experimental studies involving the effect of the size and surface density of bare AuNPs on the sensor response have been somewhat limited, both in number and in scope. In two separate studies, Lyon et al. investigated the sensor response to AuNPs with diameters ranging from 25 to 60 nm. They observed that the sensor response increased with the size of AuNPs; however, the increase was not consistent across their studies.[15,16] He et al. adsorbed 12 and 45 nm AuNPs onto a SiO_2-coated SPR chip and observed that 45 nm AuNPs produced a similar sensor response as 12 nm AuNPs, although the surface density of 45 nm AuNPs was smaller by a factor of 20.[17] Halpern et al. also adsorbed AuNPs having diameters in the range of 20 to 100 nm and observed that the sensor response increased with the volume of AuNPs.[18] Unlike the adsorption of bare nanoparticles, AuNPs employed in biomolecular detection assays are typically functionalized with molecules that bind to the analyte (or to another molecule bound to the analyte) previously captured on the sensor surface. The affinity between the functionalized AuNPs and the sensor is influenced by several conditions at the surface (Coulombic interactions, steric effects, stability of the complex with an analyte), all of which may influence the binding of

Received: July 17, 2014
Accepted: September 16, 2014
Published: September 16, 2014

   dx.doi.org/10.1021/ac502637u | *Anal. Chem.* 2014, 86, 10350−10356

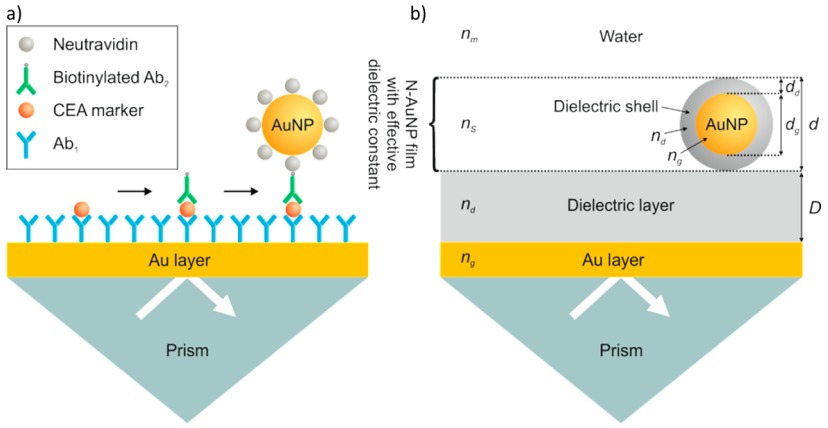

Figure 1. (a) Scheme of the experiment: sandwich assay for the N-AuNP-enhanced detection of CEA. (b) Theoretical representation—multilayer structure described by multiple refractive indexes (n_g, n_d, n_S, n_m) and thicknesses of the layers (D, d).

AuNPs on a surface of SPR biosensor.[13] The affinity binding of AuNPs of varying sizes has been reported only in a limited number of SPR studies,[11,19,20] which due to these complexities produced results which are difficult to draw universal conclusions from. While the studies performed by Uludag and Tothill[11] and Albers et al.[20] led to the conclusion that larger AuNPs produce a higher sensor response enhancement, Mitchell et al. observed no significant difference between the sensor response enhancement when using AuNPs with diameters ranging from 25 to 50 nm.[19] This suggests that the role the size of AuNPs plays in the interaction with an SPR surface is not fully understood.

In this paper, we investigate the ability of functionalized AuNPs to enhance the response of an SPR biosensor in a biomolecular detection assay, with special attention given to the study of the effect of the size of AuNPs. The sensor response (a shift in the SPR wavelength, $\Delta\lambda_r$) is studied in terms of two aspects: the surface density of captured AuNPs ($\Delta\sigma$) and the sensor sensitivity to AuNP surface density (S_σ) which are related as follows:

$$\Delta\lambda_r = \Delta\sigma \cdot S_\sigma \tag{1}$$

The first aspect ($\Delta\sigma$) is defined by the ability of the functionalized AuNPs to bind to the SPR sensor surface (the interaction of the functionalized AuNPs with the target molecule). This aspect is investigated in a model experiment in which a cancer biomarker (carcinoembryonic antigen, CEA) is detected using an SPR biosensor in a sandwich detection format. Specifically, neutravidin-functionalized AuNPs (N-AuNPs) of different sizes are used to enhance the sensor response to CEA via a biotinylated secondary antibody (Figure 1a). The second aspect (S_σ) is defined only by the optical properties of both the functionalized N-AuNPs and the properties of the sensor. This aspect represents the ratio between changes in the sensor response to changes in the N-AuNP surface density. To offer a better insight into this aspect, we present a new analytical theory describing the relationship between S_σ and the parameters of the experimental setup based on both perturbation theory,[21] which is used to describe the sensitivity to surface refractive index changes of a multilayer structure (Figure 1b), and the theory of an effective dielectric constant of a film consisting of randomly distributed nanoparticles.[22] Compared to previous theoretical studies concerning the effect of the presence of AuNPs on the optical response of an SPR sensor,[22,23] the model presented here provides an analytical formula that makes it possible to quantify the effects of parameters directly related to the experiment and, furthermore, allows for the design of an experimental system providing optimal performance.

MATERIALS AND METHODS

Reagents. Sodium acetate buffer solution, 3 M, pH 5.2 (25 °C), KH_2PO_4, Na_2HPO_4, KCl, NaCl, ethanolamine, bovine serum albumin (BSA), streptavidin, and glutaraldehyde were purchased in molecular biology grade or higher from Sigma-Aldrich, USA. *N*-Hydroxysuccin imide (NHS) and 1-ethyl-3-(3-(dimethylamino)propyl) carbodiimide hydrochloride (EDC) were purchased from GE Healthcare, USA. Primary IgG1-type antibody (Ab_1) against CEA, biotinylated secondary IgG1-type antibody (Ab_2) against CEA, and CEA were purchased from Fitzgerald, USA. Carboxy-terminated [HS−$(CH_2)_{11}$−EG_6−OCH_2−COOH] and hydroxy-terminated [HS−C_{11}−EG_4−OH] alkanethiols were purchased from Prochimia, Poland. Ethanol for spectroscopy (purity 99.9% or greater) was purchased from Merck, USA. The composition of phosphate buffer (PBS) was 1.4 mM KH_2PO_4, 8 mM Na_2HPO_4, 2.7 mM KCl, and 137 mM NaCl, pH 7.4 at 25 °C. PBS_{NaCl} consisted of phosphate buffer with the addition of 750 mM NaCl. PBS_{BSA} buffer was prepared by adding BSA to PBS to reach a concentration of 250 μg/mL. SA_{10} consisted of 10 mM sodium acetate, pH 5 at 25 °C. All buffers were prepared using deionized water (18 MΩ/cm resistivity, Direct-Q from Millipore).

Gold Nanoparticles. Spherical AuNPs covalently functionalized with neutravidin via a 2 nm polymer bridge were purchased from Nanopartz Inc., USA. The diameters of the gold core of N-AuNPs were calculated as (10 ± 2), (15 ± 2), (21 ± 2), (33 ± 1), and (52 ± 3) nm via scanning electron microscopy (SEM). These N-AuNPs were highly purified upon purchase; however, for precautionary measures, we washed them with PBS_{BSA} in order to remove any potentially free neutravidin from the solution prior to the SPR experiments. The N-AuNPs were centrifuged once for the 10 and 15 nm N-AuNPs (at 12 500 rpm for 30 min) and five times for the 21, 33, and 52 nm N-AuNPs (at 10 000 rpm for 15 min). Between the centrifugation cycles, the supernatant liquid was removed and the pellet was dissolved in 1 mL of PBS_{BSA}. After the last washing cycle, solutions of N-AuNPs were diluted in PBS_{BSA} to reach an optical density of 0.1 for the 10 and 15 nm N-AuNPs and 0.3 for the 21, 33, and 52 nm N-AuNPs (maximum of UV

dx.doi.org/10.1021/ac502637u | *Anal. Chem.* 2014, 86, 10350−10356

absorbance peak, 1 mm optical path length). The optical densities of N-AuNPs were measured using a NanoPhotometer Pearl UV−vis absorption spectrometer (Implen, Germany). The concentrations of N-AuNPs were calculated to be 10.5 (2.6 or 16.7 nM for the control experiment), 3.1, 3.4, 0.9, and 0.2 nM (0.11 or 0.45 nM for the control experiment) for N-AuNPs of the diameters of 10, 15, 21, 33, and 52 nm, respectively. The extinction coefficients (obtained from Nanopartz Inc.) for the 10, 15, 21, 33, and 52 nm N-AuNPs were 9.5×10^7, 3.2×10^8, 8.8×10^8, 3.3×10^9, and 1.5×10^{10} M^{-1} cm^{-1}, respectively.

SPR Biosensor. A laboratory four-channel SPR platform based on the wavelength spectroscopy of surface plasmons (Plasmon IV)[21] using dispersionless microfluidics[24,25] developed at the Institute of Photonics and Electronics, Czech Republic, was used in this study. In this type of SPR sensor, the angle of incidence of the light beam is fixed and the SPR dip is observed in the spectrum of light coupled to a surface plasmon. The sensor response is expressed in terms of the wavelength at which the SPR dip occurs (SPR wavelength). This response is sensitive to changes in the refractive index caused by the binding of molecules to the surface of an SPR chip. A shift of 1 nm in the SPR wavelength represents a change in the protein surface coverage of 17 ng/cm^2.[10] SPR chips were prepared by coating BK7 glass substrates with thin layers of titanium (1−2 nm) and gold (48 nm) via e-beam evaporation in vacuum.

The SPR chips used in this work were functionalized with a self-assembled monolayer of mixed carboxy-terminated and hydroxy-terminated alkanethiols, on which antibodies were immobilized using the covalent coupling as described previously.[10] A brief description of the immobilization process is provided below. Initially, a 3:7 mixture of HS−$(CH_2)_{11}$−$(EG)_6$−OCH_2−COOH and HS−C_{11}−$(EG)_4$−OH thiols was dissolved in ethanol at a total concentration of 0.2 M. A clean SPR chip was immersed in the thiol mixture for 10 min at 40 °C and stored at a room temperature for at least 12 h. Then, the chip was rinsed with ethanol and deionized water and mounted into the SPR sensor. SA_{10} buffer was flowed along the SPR chip surface for 5 min, after which the chip surface was incubated in 0.5 M NHS/0.1 M EDC (dissolved in SA_{10}) for 10 min to activate the carboxyl groups. After the activation, Ab_1 at a concentration of 10 μg/mL (67 nM) in SA_{10} was injected for 15 min to achieve a maximum surface coverage level. After short injection of SA_{10}, PBS_{NaCl} was pumped for 5 min to remove the noncovalently bound Ab_1. After another short injection of SA_{10}, 1 mM aqueous ethanolamine (pH 8 at 25 °C) was flowed along the sensor surface for 5 min to deactivate any remaining carboxyl groups.

SPR Experiments. The effect of the AuNPs size on the SPR sensor response was studied in a model sandwich assay for the detection of CEA. A scheme of this assay is shown in Figure 1a.

In a typical SPR experiment, all four channels (two detection and two reference channels) were used to measure the binding of two different sizes of N-AuNPs. In each detection channel, CEA, Ab_2, and N-AuNPs were consecutively injected to form the sandwich, while in the reference channel all the assay steps were performed except for the injection of CEA. Specific steps were as follows. Prior to the detection of CEA, the sensor surface with immobilized Ab_1 was incubated in PBS_{BSA} for 15 min. Then, CEA at a concentration of 500 ng/mL (2.5 nM) in PBS_{BSA} and PBS_{BSA} was injected for 10 min through the detection and reference channels, respectively. After a short injection of PBS_{BSA}, Ab_2 (10 μg/mL, 67 nM) was pumped through both the detection and reference channels for 15 min. After another short injection of PBS_{BSA}, solutions of N-AuNPs were flowed through both channels. In order to capture the maximum amount of N-AuNPs (and achieve a maximum enhancement), the concentrations of N-AuNPs in each SPR experiment were preselected to maximize the sensor response obtained within a time frame of several hours, such that the N-AuNP surface density had approached an equilibrium state. Finally, the solution of N-AuNPs was replaced with PBS_{BSA}.

An additional experiment was carried out to confirm the long-term stability of the Ab_1-CEA-Ab_2 complex. In this experiment, a rather high concentration of CEA (1000 ng/mL) was used, and after the formation of Ab_1-CEA-Ab_2, PBS_{BSA} was pumped through the sensing channel for several hours, while the sensor response was recorded. For the determination of kinetic and equilibrium constants, CEA at concentrations of 250, 500, 1500, and 5000 ng/mL in PBS_{BSA} were injected into the parallel channels of the SPR sensor and flowed over the antibody-coated surface for 10 min. Then, PBS_{BSA} was pumped for 20 min to obtain the dissociation phase of the interaction. The kinetic constants were determined with BIAevaluation software (Biacore, version 4.1) using a 1:1 Langmuir model, which also considered mass transport effects. It should be noted that all SPR experiments reported in this work used a flow rate and temperature of 20 μL/min and 25 °C, respectively.

SEM Measurements. After the SPR experiments, the SPR chips were analyzed via SEM (e_LiNE plus system produced by Raith, Germany) in order to determine the diameter and surface density of the N-AuNPs on the SPR chip surface. In order to avoid any loss of N-AuNPs from the surface of an SPR chip during the transition from the SPR sensor to the SEM, the N-AuNPs were covalently immobilized to the surface of the SPR chip via glutaraldehyde. The immobilization was performed as follows. PBS_{BSA} was replaced with SA_{10}, and 2.5% (v/v) glutaraldehyde in SA_{10} was injected for 30 min to cross-link the amino-groups of molecules on the surface of SPR chip. Then, SA_{10} was again injected. Before the removal of a chip from the SPR biosensor, Q water was flowed through the flow-cell to remove any residual salts from the surface of the SPR chip.

The diameter and surface density of N-AuNPs on the SPR chip surface were determined from SEM images collected by an e_LiNE plus system by means of an in-lens secondary electron detector and a 10 kV acceleration voltage. Surface densities were calculated using the public domain software ImageJ (http://imagej.nih.gov/ij/). The images (10 μm × 10 μm) were taken from five different spots across each channel.

RESULTS AND DISCUSSION

SPR Sensor Response to N-AuNPs. In order to characterize the enhancement of the sensor response due to the capture of N-AuNPs, we utilized the sandwich assay shown in Figure 1a. A typical sensorgram showing the sensor response in different stages of the assay is shown in Figure 2. The injection of CEA ($K_{D(CEA)} = 3.3 \times 10^{-10}$ M; see Figure S-1 in the Supporting Information) gave rise to a sensor response that increased linearly with time, reaching a value of 0.45 ± 0.05 nm after 10 min (measured across all experiments). This injection time was limited in order to obtain a sensor surface having a low CEA surface density as to minimize potential effects related to crowding. We determined that the surface density of CEA (M = 200 kDa) was 228 CEA/μm^2, which implied that only 2.9% of the Ab_1 (the response of 12 nm, M = 150 kDa) was occupied by CEA. The response to the secondary antibody was

dx.doi.org/10.1021/ac502637u | Anal. Chem. 2014, 86, 10350−10356

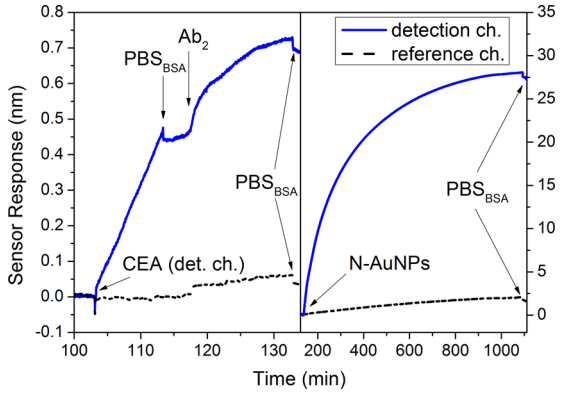

Figure 2. Sensor response obtained during a typical CEA assay using 33 nm N-AuNPs.

found to increase with time, reaching a plateau of 0.17 ± 0.03 nm in 15 min. The subsequent time-response to N-AuNPs was dependent on the size of N-AuNPs and varied from several nanometers to several tens of nanometers. The nonspecific binding of N-AuNPs in a reference channel (caused by both the adsorption of N-AuNPs to the SPR chip surface and by specific binding of N-AuNPs to nonspecifically bound biotinylated Ab_2) was in each case lower than 10% of the enhanced sensor response obtained in the detection channel. Therefore, the nonspecific binding of N-AuNPs had a rather minor effect on the outcome of the experiments considering the much higher specific sensor response.

Using the results of each detection experiment, we calculated the equilibrium sensor response ($\Delta\lambda_r$) as the difference between the sensor response of the detection and the reference channels, where $\Delta\lambda_r$ thus describes the sensor response to only the specifically bound N-AuNPs. The values of $\Delta\lambda_r$ obtained for the 5 different sizes of N-AuNPs are shown in Figure 3.

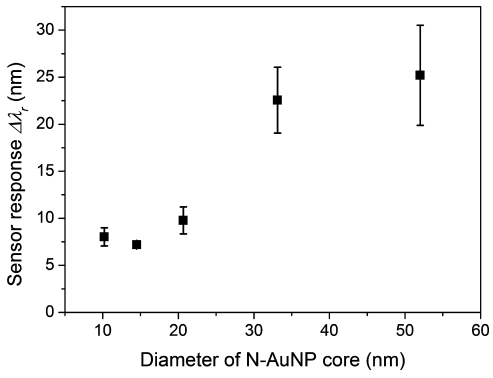

Figure 3. Sensor responses, $\Delta\lambda_r$, for N-AuNPs with diameters of the gold core of 10, 15, 21, 33, and 52 nm. Errors were calculated as the standard deviation from at least three measurements regarding different SPR chips.

The $\Delta\lambda_r$ values obtained for the two smallest N-AuNPs did not differ considerably, and the $\Delta\lambda_r$ values of the three smallest N-AuNPs were much lower than the $\Delta\lambda_r$ values observed for the two largest N-AuNPs. Specifically, the 52 nm diameter N-AuNPs generated a $\Delta\lambda_r$ value 3.5 times higher than that observed when using 15 nm N-AuNPs. The trend of higher $\Delta\lambda_r$ values obtained with larger AuNPs is in agreement with results published in Uludag and Tothill[11] and Albers et al.[20] As follows from Figure 3, the relative standard deviation of $\Delta\lambda_r$ tends to increase with increasing diameter of N-AuNPs. We believe that this is mainly due to the greater ability of bigger AuNPs to enhance the differences among different experiments.

We also performed control experiments where we evaluated (i) the effect of different concentrations of N-AuNPs (for the same nanoparticle size) and (ii) the long-term stability of the Ab_1-CEA-Ab_2 complex. Regarding (i), we investigated whether $\Delta\lambda_r$ was independent of the concentration of the injected N-AuNPs. We pumped 2.6 and 16.7 nM solutions of 10 nm N-AuNPs and 0.11 and 0.44 nM solutions of 52 nm N-AuNPs across the surface with immobilized Ab_2 at a constant surface coverage (see Figure S-2 in the Supporting Information). Note here that these two N-AuNP concentrations were chosen to be lower and higher than the respective concentrations used in the main SPR experiment (10.5 and 0.2 nM for 10 and 52 nm N-AuNPs, respectively). From Figure S-2 in the Supporting Information, it can be seen that the obtained $\Delta\lambda_r$ values were approximately the same for both N-AuNP concentrations, for both diameters (10 and 52 nm). Therefore, we concluded that the $\Delta\lambda_r$ values have rather low dependence on the particle concentration (where the N-AuNP concentration used herein is well above the equilibrium dissociation constant of the Ab_2/N-AuNP affinity complex). Regarding the long-term stability of the Ab_1-CEA-Ab_2 complex (ii), buffer was flowed across the sensor surface with the Ab_1-CEA-Ab_2 complex for several hours and the dissociation phase of the bound CEA-Ab_2 complex was observed (see Figure S-3 in the Supporting Information). This experiment revealed that Ab_2 does not dissociate from the surface of an SPR chip (in appreciable amounts during the time scales involved within this study) and confirmed that the stability of the Ab_1-CEA-Ab_2 complex is not of concern here.

Surface Density of N-AuNPs. The surface densities ($\Delta\sigma$) of N-AuNPs for each measurement were obtained via SEM images as the difference between the densities measured in the detection and reference channels (see Figure 4). The mean values of surface densities $\Delta\sigma$ were found to be 106.1, 53.2, 19.9, 15.0, and 3.9 N-AuNPs/μm^2 for the diameters of 10, 15, 21, 33, and 52 nm, respectively. From the SPR sensor response to the biotinylated secondary antibody, we estimated the surface density of Ab_2 to be 116 $Ab_2/\mu m^2$. Assuming that the N-AuNP/Ab_2 obeys a 1:1 affinity interaction, we estimated that 91.5% and 3.4% of Ab_2 were occupied by the smallest and largest N-AuNPs, respectively.

As follows from the SEM measurements (Figure 4), the dependence of $\Delta\sigma$ on the size of the N-AuNPs was rather dramatic: $\Delta\sigma$ for the 10 nm N-AuNPs was 27 times larger than that observed for the 52 nm N-AuNPs. This remarkable difference cannot be explained by the blocking of the N-AuNP binding due to the closely packed arrangement of N-AuNPs on a chip surface. We estimate that the surface coverage was only about 0.8% for both 10 and 52 nm N-AuNPs, which offered ample room for the capture of additional N-AuNPs. This steep decrease in $\Delta\sigma$ cannot be explained by the difference in concentrations of N-AuNPs, as we observed only very low sensitivity of $\Delta\lambda_r$ to the variations in the concentration of N-AuNP (see above). Therefore, we hypothesize that this effect of N-AuNP size on $\Delta\sigma$ was caused by (a) steric effects that influenced the accessibility of biotin for binding to the N-AuNPs, (b) binding of several N-AuNPs to multiple biotins on a single Ab_2, and (c) binding of one N-AuNP to one or more biotins on multiple Ab_2 antibodies. These effects will be explored below.

dx.doi.org/10.1021/ac502637u | Anal. Chem. 2014, 86, 10350−10356

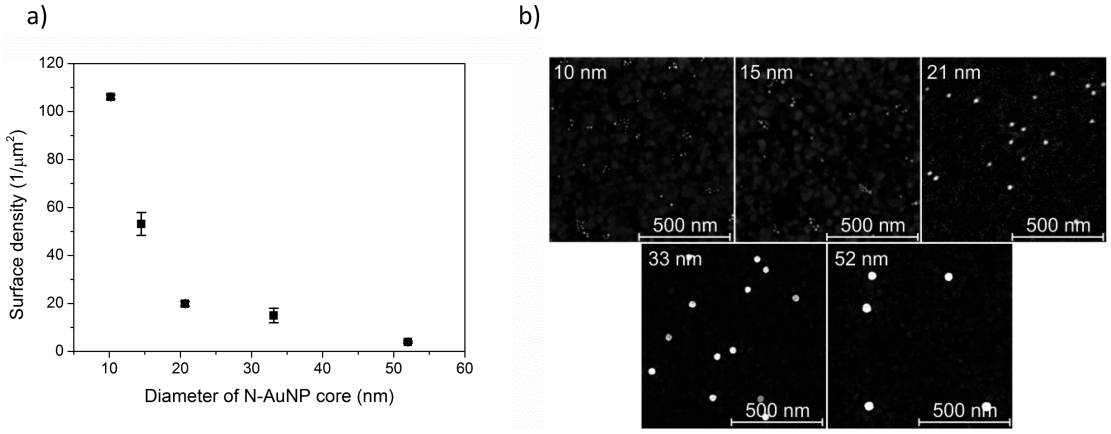

Figure 4. (a) Surface densities obtained for five different N-AuNP sizes. Errors were calculated as the standard deviation from three different chips, where five spots were measured across each chip. (b) SEM images of the surface of an SPR chip with N-AuNPs of different sizes.

To investigate the role of steric effects on the binding of N-AuNPs on the surface of an SPR chip (a), we carried out an experiment in which the incubation of the surface with the largest 52 nm N-AuNPs was followed by the injection of the smallest 10 nm N-AuNPs (Figure 5). The sensor exhibited a

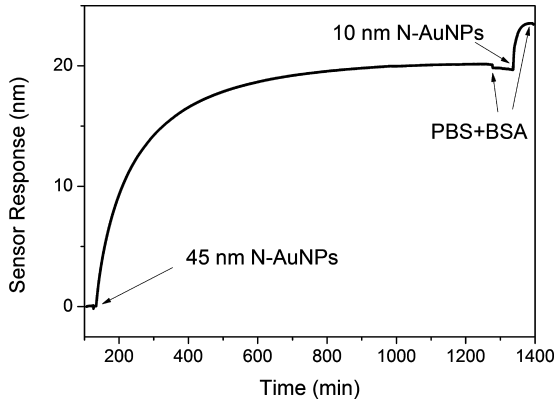

Figure 5. Reference compensated sensor response to the injection of 0.2 nM, 52 nm N-AuNPs followed by the injection of 10.5 nM, 10 nm N-AuNPs.

$\Delta\lambda_r$ value of 20 nm to the injection of the 52 nm N-AuNPs and was followed by a response of 4 nm to the 10 nm N-AuNPs. This additional binding of the 10 nm N-AuNPs demonstrated that there were unoccupied biotins still present on the surface of an SPR chip, and furthermore, these unoccupied sites remained active for the interaction with additional N-AuNPs. Quantitatively, the amount of unoccupied biotin sites after incubation with the 52 nm N-AuNPs was approximately 50% of the originally accessible biotin. This experiment clearly demonstrated that the accessibility of biotins for N-AuNP binding was higher for the smaller N-AuNPs and, furthermore, provides a partial explanation for the strong effect that the N-AuNP size has on $\Delta\sigma$ seen in Figure 4a. This hypothesis was also supported by another experiment in which streptavidin was pumped along the surface of the SPR chip prior to the injection of N-AuNPs (data are not shown). We estimated that each Ab_2 was able to bind approximately three streptavidins. In comparison, this binding capacity was higher by a factor of 3 and 6 with respect to $\Delta\sigma$ values of the 10 and 15 nm N-AuNPs, respectively.

In regards to (b), the observed $\Delta\sigma$ may have also been affected by the binding of several N-AuNPs to a single Ab_2. Although we do not know the exact volume occupied by each Ab_2, the typical dimensions of an antibody vary from 15 to 20 nm in length, from 6 to 15 nm in width, and from 6 to 10 nm in height.[11] These dimensions suggest that the probability of multiple N-AuNP binding events to a single Ab_2 will increase with a decrease in the size of the N-AuNP, in particular for the smallest N-AuNPs used in this study. Therefore, it is likely that this effect will lead to an increase in $\Delta\sigma$ for smaller N-AuNPs.

In regards to (c), the possible binding of one N-AuNP to one or more biotins on multiple Ab_2 antibodies, assuming the above stated dimensions of Ab_2 (specifically the average footprint: 18 nm × 10 nm), the coverage of Ab_2 was estimated to be about 2%, having an average distance between homogeneously distributed Ab_2 of approximately 77 nm. In reality, the distribution of Ab_2 on the surface is random and the real distance between Ab_2 will be much smaller, allowing for the possibility of a larger N-AuNP to bind to biotin sites on multiple Ab_2. As follows, it is likely that this effect will lead to a decrease in $\Delta\sigma$ for larger N-AuNPs.

Sensitivity to Surface Density of AuNPs. Experimental values of S_σ (Figure 6) were obtained by dividing the equilibrium sensor response $\Delta\lambda_r$ (Figure 3) by the surface density $\Delta\sigma$ determined by SEM measurements (Figure 4) for each N-AuNP size.

Below, we present an analytical theory describing the experimental system. The multilayer structure that we consider is shown in Figure 1b, which consists of a gold layer ($n_g = (\varepsilon_g)^{1/2} = 0.138 + 4.49i$ at $\lambda_r = 750$ nm[26]), a thin dielectric layer representing a self-assembled monolayer of alkylthiols with immobilized biorecognition elements ($D = 10$ nm, $n_d = (\varepsilon_d)^{1/2} = 1.42$[27]), a layer composed of randomly distributed N-AuNPs of overall thickness d surrounded in aqueous medium, and the aqueous medium ($n_m = (\varepsilon_m)^{1/2} = 1.33$). N-AuNPs were simulated as core−shell particles, composed of a gold core with a diameter d_g and a dielectric shell representing the linker layer and biomolecules attached to the surface of the AuNP ($d_d = 10$ nm). The effective dielectric constant of the layer of N-AuNPs $\varepsilon_S = n_S^2$ was simulated using the theory of optical properties of materials consisting of randomly distributed nanoparticles at low surface coverage[22] and can be written as

$$\varepsilon_S = \varepsilon_m\left(1 + \frac{\sigma\alpha}{d}\right) \quad (2)$$

dx.doi.org/10.1021/ac502637u | Anal. Chem. 2014, 86, 10350−10356

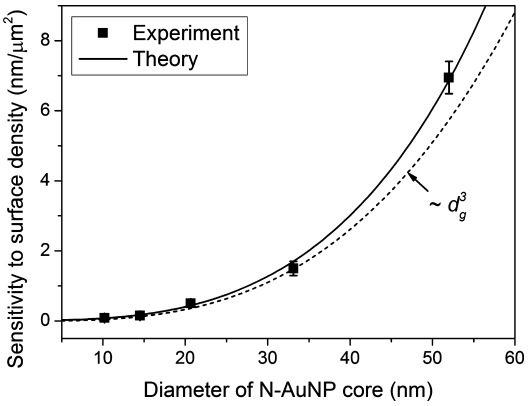

Figure 6. Theoretical (calculated using eq 6) and experimental sensor sensitivity S_σ to surface density as a function of N-AuNP size. The dotted line represents a cubic dependence of S_σ on the AuNP diameter calculated by the simplified model using eq 7. The error bars are the propagated standard deviation from the results shown in Figures 3 and 4.

where σ and α are the surface density and polarizability of the N-AuNP, respectively. If the N-AuNP size is smaller than the wavelength of the incident light, we can apply the electrostatic approximation,[28] where the polarizability of the N-AuNP is expressed as

$$\alpha = \pi d^3 \frac{\varepsilon - \varepsilon_m}{6\varepsilon_m + 2(\varepsilon - \varepsilon_m)F} \tag{3}$$

where ε is the effective dielectric constant of the core−shell particle,[28] $\varepsilon = \varepsilon_d[1 + 3\beta/(1 - \beta)]$, with $\beta = f(\varepsilon_g - \varepsilon_d)/(3\varepsilon_d + (\varepsilon_g - \varepsilon_d))$, and $f = d_g^3/(d_g + 2d_s)^3$ is the fraction of the total particle volume occupied by the gold core. The factor $F = 1 - F_1 - F_2 - F_3$ includes three correction terms which take into account the dynamic depolarization $F_1 = (kd)^2/4$, radiative damping ($F_2 = i(kd)^3/12$),[29] and the influence of the presence of the gold layer $F_3 = (1/4)[d/(2D^* + d)]^3((\varepsilon_g - \varepsilon_m)/(\varepsilon_g + \varepsilon_m))$, $D^* = (D\varepsilon_d)/\varepsilon_m$ (approximation for high angles of incidence).[30]

The sensitivity of an SPR sensor (based on wavelength modulation) to changes in the surface density of N-AuNPs can be written as

$$S_\sigma = \frac{d\lambda_r}{d\sigma} = \frac{d\lambda_r}{dn_S}\frac{dn_S}{d\varepsilon_S}\frac{d\varepsilon_S}{d\sigma} = \frac{S_S}{2n_m}\frac{d\varepsilon_S}{d\sigma} \tag{4}$$

where $S_S = d\lambda_r/dn_S$ is the sensitivity to refractive index changes within the layer containing the randomly distributed N-AuNPs. As follows from perturbation theory,[22] the sensitivity S_S can be expressed as $S_S = S_B I_S d$, where $S_B = (d\lambda_r/dn_m)$ is the sensitivity to bulk refractive index changes (S_B = 4081 nm/RIU for λ_r = 750 nm). The term I_s is a factor reflecting the exponential profile of the surface plasmon field and can be written as

$$I_S = \frac{1 - \exp(-2d/L_{pd})}{d} \tag{5}$$

where L_{pd} is the penetration depth of the surface plasmon (L_{pd} = 275 nm for λ_r = 750 nm). By applying the perturbation theory and eq 2 and further neglecting the effect of the imaginary part of α, eq 4 can be reduced to

$$S_\sigma = \frac{n_m}{2} S_B I_S Re\{\alpha\} \tag{6}$$

As follows from eq 6, S_σ is directly proportional to (i) the bulk sensitivity S_B that describes the sensitivity of the sensor to refractive index changes, (ii) the factor I_S that accounts for the profile of the surface plasmon field (the I_S factor decreases with the size of the N-AuNPs), and (iii) the real part of the particle polarizability $Re\{\alpha\}$. The term $Re\{\alpha\}$ depends on the size and composition of the N-AuNPs, the distance of the N-AuNPs from the metal layer surface, and the incident wavelength. Specifically, for wavelengths longer than the localized surface plasmon resonance (LSPR) wavelength of a N-AuNP, $Re\{\alpha\}$ increases with the N-AuNP size, while the opposite trend holds for wavelengths shorter than the LSPR.[22]

In the special cases such that the N-AuNPs are rather distant from the surface ($d \ll D$, $F_3 \approx 0$), the effect of their shell is negligible ($\varepsilon \approx \varepsilon_g$); furthermore, if their size is much smaller that the incident wavelength ($d \ll \lambda_r$, $F_1 \approx F_2 \approx 0$), the real part of polarizability $Re\{\alpha\}$ increases with d_g^3. Additionally, if the diameter of N-AuNPs is much smaller than the penetration depth of the surface plasmon ($d \ll L_{pd}$), I_S can be reduced to $I_S \approx 2/L_{pd}$ (becoming independent of d), and the model can be simplified to

$$S_\sigma \approx \pi d_g^3 \frac{S_B n_m}{L_{pd}} Re\left\{\frac{(\varepsilon_g - \varepsilon_m)}{6\varepsilon_m + 2(\varepsilon_g - \varepsilon_m)}\right\} \tag{7}$$

where sensitivity S_σ is proportional to d_g^3.

Figure 6 shows S_σ calculated for a range of AuNP diameters using eq 6 (solid line) and eq 7 (dashed line). It can be seen that for very small N-AuNPs (until the diameter of N-AuNP core reaches about 20 nm) the simplified model (eq 7) provides accurate prediction and the sensitivity of the SPR sensor to N-AuNPs increases with approximately the third power of the diameter of the N-AuNP core. With further increases in the diameter of N-AuNPs core, the simplified model yields underestimated values; the faster growth of S_σ for larger N-AuNPs is a consequence of dynamic depolarization, radiative damping, the influence of the presence of the gold layer, and the fact the SPR wavelength is much longer than the LSPR wavelength of the N-AuNPs. The theoretical model described by eq 6 (solid line) is in excellent agreement with the experimental data throughout the whole range of AuNP diameters.

CONCLUSIONS

In this paper, we describe, both theoretically and experimentally, the ability of gold spherical NPs to enhance the sensitivity of SPR biosensors. The effect of NPs on the response of SPR sensor was experimentally studied using gold nanoparticles functionalized with neutravidin (N-AuNPs) in a model sandwich assay for the detection of carcinoembryonic antigen (CEA). The detection experiments combined with the characterization of each SPR chip using electron microscopy revealed that the observed sensor response enhancement is determined by two factors: sensor sensitivity to N-AuNP surface density (the response of the sensor to the single nanoparticle per unit surface, S_σ) and the ability of the N-AuNPs to bind functionalized sensor surface. Both these factors were found to have dependence on the size of the N-AuNPs; while the pure optical enhancement was found to increase with the size of N-AuNPs, the number of N-AuNPs bound to the SPR chip surface followed an opposite trend. To our knowledge, this represents the first time that the effect of the AuNP size on its ability to bind to target molecules on the

dx.doi.org/10.1021/ac502637u | Anal. Chem. 2014, 86, 10350−10356

sensor surface has been observed and quantified in SPR biosensor-based biodetection experiments. In addition, our findings suggest that this effect can be potentially significant and should be taken into account when planning the use of NPs to enhance the sensitivity of an SPR sensor. These results should stimulate and guide research into surface functionalization toward functional sensor surfaces and NPs harnessing the full enhancement potential of NPs predicted by theory.

A theoretical model has been established that describes the SPR sensor response due to the presence of the NPs. The model provides an analytical formula that relates S_σ with measurable characteristics of the NPs (composition, size) and geometry (distance of NPs from the surface of the SPR chip). This formula offers a simple means for predicting the enhancement of the sensor response for specific NPs, including variable experimental geometries, and provides a better understanding of the roles that pertinent experimental parameters may play. Special attention was paid to the role of the diameter of the NPs, and we described the conditions under which the enhancement follows the intuitive trend of scaling with the volume of the NP and, furthermore, how (potentially substantially) the enhancement may differ outside these conditions. The dependence of the optical enhancement on the size of N-AuNP provided by the theoretical model was in excellent agreement with the experimental data. Although the theory presented herein was developed for SPR biosensors, it can be adopted to different types of optical biosensors and expanded to a wide variety of sensor sensitivity enhancing NPs.

■ ASSOCIATED CONTENT

Supporting Information

Control experiments. This material is available free of charge via the Internet at http://pubs.acs.org.

■ AUTHOR INFORMATION

Corresponding Author

*E-mail: homola@ufe.cz.

Notes

The authors declare no competing financial interest.

■ ACKNOWLEDGMENTS

We thank N. S. Lynn for valuable comments and discussions. This research was supported by Praemium Academiae of the Academy of Sciences of the Czech Republic, the Czech Science Foundation (Contract # P205/12/G118) and by the US Army Research Office (Contract # W911NF-13-1-0460).

■ REFERENCES

(1) Homola, J. *Chem. Rev.* **2008**, *108*, 462−493.
(2) Su, F.; Xu, C.; Taya, M.; Murayama, K.; Shinohara, Y.; Nishimura, S. I. *Sensors* **2008**, *8*, 4282−4295.
(3) Chung, J. W.; Park, J. M.; Bernhardt, R.; Pyun, J. C. *J. Biotechnol.* **2006**, *126*, 325−333.
(4) Teramura, Y.; Iwata, H. *Anal. Biochem.* **2007**, *365*, 201−207.
(5) Kim, M. G.; Shin, Y. B.; Jung, J. M.; Ro, H. S.; Chung, B. H. *J. Immunol. Methods* **2005**, *297*, 125−132.
(6) Cao, C.; Sim, S. J. *J. Microbiol. Biotechnol.* **2007**, *17*, 1031−1035.
(7) Kubitschko, S.; Spinke, J.; Bruckner, T.; Pohl, S.; Oranth, N. *Anal. Biochem.* **1997**, *253*, 112−122.
(8) Teramura, Y.; Arima, Y.; Iwata, H. *Anal. Biochem.* **2006**, *357*, 208−215.
(9) Huang, L.; Reekmans, G.; Saerens, D.; Friedt, J. M.; Frederix, F.; Francis, L.; Muyldermans, S.; Campitelli, A.; Van Hoof, C. *Biosens. Bioelectron.* **2005**, *21*, 483−490.
(10) Springer, T.; Homola, J. *Anal. Bioanal. Chem.* **2012**, *404*, 2869−2875.
(11) Uludag, Y.; Tothill, I. E. *Anal. Chem.* **2012**, *84*, 5898−5904.
(12) Schneider, B. H.; Dickinson, E. L.; Vach, M. D.; Hoijer, J. V.; Howard, L. V. *Biosens. Bioelectron.* **2000**, *15*, 13−22.
(13) Bedford, E. E.; Spadavecchia, J.; Pradier, C. M.; Gu, F. X. *Macromol. Biosci.* **2012**, *12*, 724−739.
(14) Kwon, M. J.; Lee, J.; Wark, A. W.; Lee, H. J. *Anal. Chem.* **2012**, *84*, 1702−1707.
(15) Lyon, L. A.; Pena, D. J.; Natan, M. J. *J. Phys. Chem. B* **1999**, *103*, 5826−5831.
(16) Lyon, L. A.; Musick, M. D.; Smith, P. C.; Reiss, B. D.; Pena, D. J.; Natan, M. J. *Sens. Actuators, B: Chem.* **1999**, *54*, 118−124.
(17) He, L.; Smith, E. A.; Natan, M. J.; Keating, C. D. *J. Phys. Chem. B* **2004**, *108*, 10973−10980.
(18) Halpern, A. R.; Wood, J. B.; Wang, Y.; Corn, R. M. *ACS Nano* **2014**, *8*, 1022−1030.
(19) Mitchell, J. S.; Wu, Y. Q.; Cook, C. J.; Main, L. *Anal. Biochem.* **2005**, *343*, 125−135.
(20) Albers, W. M.; Munter, T.; Laaksonen, P.; Vikholm-Lundin, I. *J. Colloid Interface Sci.* **2010**, *348*, 1−8.
(21) Vaisocherova, H.; Zitova, A.; Lachmanova, M.; Stepanek, J.; Kralikova, S.; Liboska, R.; Rejman, D.; Rosenberg, I.; Homola, J. *Biopolymers* **2006**, *82*, 394−398.
(22) Uchiho, Y.; Shimojo, M.; Furuya, K.; Kajikawa, K. *J. Phys. Chem. C* **2010**, *114*, 4816−4824.
(23) Golden, M. S.; Bjonnes, A. C.; Georgiadis, R. M. *J. Phys. Chem. C* **2010**, *114*, 8837−8843.
(24) Springer, T.; Piliarik, M.; Homola, J. *Sensor Actuat B-Chem.* **2010**, *145*, 588−591.
(25) Springer, T.; Piliarik, M.; Homola, J. *Anal. Bioanal. Chem.* **2010**, *398*, 1955−1961.
(26) Johnson, P. B.; Christy, R. W. *Phys. Rev. B* **1972**, *6*, 4370−4379.
(27) Malinsky, M. D.; Kelly, K. L.; Schatz, G. C.; Van Duyne, R. P. *J. Am. Chem. Soc.* **2001**, *123*, 1471−1482.
(28) Bohren, C. F. Huffman, D. R. *Absorption and Scattering of Light by Small Particles*; John Wiley and Sons: New York, 1983.
(29) Jensen, P. *Rev. Mod. Phys.* **1999**, *71*, 1695−1735.
(30) Pinchuk, A.; Hilger, A.; von Plessen, G.; Kreibig, U. *Nanotechnology* **2004**, *15*, 1890−1896.